

Evaluation of Impurity Migration and Microwave Digestion Methods for Lithographic Materials

Fu-Hsiang Ko¹, Li-Tung Hsiao², Cheng-Tung Chou², Mei-Ya Wang³, Tien-Ko Wang³, Yuh-Chang Sun⁴, Bor-Jen Cheng⁵, Steven Yeng⁵ and Bau-Tong Dai¹

¹National Nano Device Laboratories, National Chiao Tung University, Hsinchu 300, Taiwan

²Department of Chemical Engineering, National Central University, Chung-Li, Taoyuan 320, Taiwan

³Department of Engineering and System Science, National Tsing Hua University, Hsinchu 300, Taiwan

⁴Nuclear Science and Technology Development Center, National Tsing Hua University, Hsinchu 300, Taiwan

⁵Mosel Vitelic Inc., NO19 Li-Hsin RD., Science-Based Industrial Park, Hsinchu 300, Taiwan

ABSTRACT

In the section of incoming quality (IQC) or quality reliability analysis (QRA) of advanced semiconductor fabrication company, it is inevitable to regulate the strict standard for the incoming materials to ensure the reliability. In our radioactive tracer study, it is interestingly found the various amounts of metal and trace element impurities in the lithographic materials may migrate into the substrate. Based on the complex organic matrix in lithographic materials such as bottom anti-reflective coating (BARC), I-line resist and DUV resist, it is not easy to directly determine the multi-elements by the instrumentation. In this work, the lithographic materials are first decomposed by the close-vessel and open-focused microwave oven, and the digest is evaporated to incipient dryness. After adding water, the sample solutions are used either for evaluating the completeness of the digestion process by UV-VIS spectrometer, or for the determination of eleven elements using inductively coupled plasma mass spectrometry (ICP-MS). In addition, the digestion efficiency is also evaluated by the weight of total dry residual after various digestion recipes. By the complementary digestion method, the method detection limits for analytes can be achieved at lower than ng/g level. For evaluation of data accuracy, the results obtained by the two independent digestion methods are in good agreement. Moreover, the spiking recovery tests for all the elements are of 70 to 130%. According to the microcontamination control limit predicted by the SIA roadmap, the established method can meet the requirements for the quality control of lithographic materials in the future ten years.

Keywords: lithographic material, impurity migration, impurity determination, quality control, microwave digestion, ICP-MS determination

1. INTRODUCTION

The increasing complexity and miniaturization of modern integrated circuits demand a higher device yield and hence decreasing defect density in the active region of silicon devices¹. For a deep submicrometer device, a single metal precipitate could cause a distortion of the resultant electrical properties and may result in faulty integrated circuit²⁻⁵. For example, metals can degrade the dielectric properties of gate oxide causing premature breakdown. They can also diffuse into the bulk of the silicon substrate resulting in increased junction leakage as well as reduced minority carrier lifetime. Therefore, a better knowledge of the diffusion route and behavior of the impurities introduced into the silicon substrate during device fabrication could help to control the contamination and thus promote the circuit yield.

The control of fabrication processes involved in device manufacturing becomes more and more crucial due to increasing complexity for the materials and tools. Among them, lithography plays a very important role because it is applied repeatedly to the wafer surface during device manufacturing. Many lithographic models have been developed and applied for the photoresist profile simulation⁶⁻⁸, however, the effects of impurity diffusion regarding Cs and Zn impurities in the lithographic materials have, to the best of our knowledge, never been reported. The behavior of metallic contaminants in lithographic materials and their migration into the underlying substrate is of eminent importance, because proper control of elemental impurity levels in the "high-purity" lithographic materials would be very crucial for the fast proliferation of lithography process in the IC industry in the coming years⁹. Although it is always safer to demand an unnecessarily high degree of purity for lithographic materials, however, the resulting cost would be extremely expensive and unnecessary. As this would require tedious sample pre-treatment procedures, including matrix decomposition by hot plate or microwave oven, separation, pre-concentration, and control of sample handling and analytical environment¹⁰⁻¹².

To evaluate the ratios of metallic impurities diffusing from deep ultraviolet photoresist (DUV PR) or bottom anti-reflective coating (BARC) into the underlying substrate during lithographic processing, e.g., baking, it requires various analytical methods¹³⁻¹⁷ for determining the impurities in the resist layer and in the underlying substrate. Among these

analytical methods, radioactive tracer technique¹⁸⁻²⁰ has proved to be very suitable for studying element migration in materials, environment, and biochemistry. In semiconductor fabrication, the well-known RCA cleaning method²¹, universally applied in wafer processing for removing impurities from silicon wafer, was originally developed based on the radioactive tracer method by Kern and Puotinen in 1970. It is still in wide use today, and forms the basis of many so-called "modified RCA cleaning methods" for wafer cleaning. The effectiveness of the RCA cleaning method was first established by deliberately contaminating the wafer surface with radioactive nuclides of ⁶⁴Cu and ¹⁹⁸Au. Gamma radioactivity was then recorded before and after RCA cleaning so as to monitor the cleaning efficiency. The advantages of the radioactive tracer technique are well recognized and include high throughput, easy operation, interference-free from stable isotope and reliability. Despite the versatility of the radioactive tracer technique, however, it has not been applied to study the impurity migration during lithographic materials and the underlying substrates.

Today, the determination of ultratrace elements of lithographic materials for vendor or advanced semiconductor device manufacturing uses the graphite furnace atomic absorption spectrometry (GFAAS)²². The sample are diluted with organic solvent to a proper factor or simply digested with hot plate. However, throughput is an important issue to be challenged due to only one element can be measured in one time by the above method. Plasma-based instruments such as inductively coupled plasma mass spectrometry (ICP-MS) or inductively coupled plasma optical emission spectrometry (ICP-OES) possess the advantage of simultaneous multielement capability. However, they require rapid, efficient and reliable sample preparation technology to complement their efficiency and capability. This is because Plasma-based instrument easily suffers from matrix induced spectral overlap problems and matrix induced signal intensity changes by the incomplete sample dissolution²³⁻²⁴.

Closed-vessel microwave digestion of biological samples with acid at elevated temperature and pressure rapidly destroys the organic matrix^{12,25}. Under these conditions, the oxidizing power of the acid is significantly increased, and the contamination, loss of volatile elements and dissolution time are reduced. The limitations of the closed-vessel method are small sample size and built-in pressure, which affect the detection limit and safety. Moreover, the manifolds of the most commercial microwave ovens has a rather large irradiated space, the volume ratio of the oven to the reaction area is unfavorably high and the power absorption inefficient. The percentage of non-absorbed power with such small loads was rather high, and its reflected portion could damage the magnetron or, at least, impair its performance. On the contrary, the open-focused microwave digestion method can adopt large sample size up to 10g. The method is operating in the atmosphere, and the problem of accumulating pressure in the reaction chamber can be avoided²⁶. Moreover, it has a relatively small irradiation zone. The disadvantage of the digestion method is the probability of contamination from the ambient air, cross contamination between samples, and loss of analytes is expected to increase. To solve these problems, a quartz-made chamber and reflux condenser can be used to minimize the risk of contamination and the loss of analytes adsorbed on the container.

Lithographic materials contain the polymer and other complex matrix which have high strength and are resistant to elevated temperatures, so the dissolution method to be reported is rather few. For example, since the demand of high plasma resistant for the resist in the dry etching process of device manufacturing, the molecular weight or structure of the lithographic material has been modified to enhance its etching tolerance. However, this modification leads the material dissolution very difficult, and is unfavorable for the quality control issue. Hence, to meet the requirement of impurity quality control level now and future, the digestion recipe and the determination method for the lithographic materials remain to be developed.

In this work, the radioactive tracer method was first proposed to investigate the migration ratio of Cs and Zn impurities from DUV PR and BARC into the underlying substrate. The effects of baking temperatures were also evaluated. Possible mechanisms and the effects of various underlying surfaces for the impurity diffusion were discussed. Furthermore, the methods of total dry residual solid and UV absorption for evaluating the digestion efficiency of the lithographic materials with various microwave digestion methods and recipes were studied. The suitable digestion recipes were obtained for the determination of trace and ultratrace elements in general lithographic materials. Finally, a series of lithographic materials was selected to test the applicability of the proposed digestion method and determined by ICP-MS and ICP-OES.

2. EXPERIMENTAL

2.1 Materials

P-type <100> wafers with 15 cm in diameter were passivated with various films (i.e., polysilicon, silicon dioxide, silicon nitride, and non-passivated or bare silicon control). They were then cut into pieces, with 2 cm by 2 cm in area, to serve as test samples. These test samples were processed through various lithographic processes to study the contaminants as introduced by the lithographic process Carrier-free radioactive tracers from DAMRI (France) were used in this study. Their composition was 10 µg/g of ¹³⁷CsCl (0.747 M Bq/g) and 10 µg/g of ⁶⁵ZnCl₂ (0.857 M Bq/g) in 0.1 N hydrogen chloride solution.

The lithographic materials used in this work was DUV PR of AZ DX-2034P (Clariant, Japan), i-line PR (Japan

Synthesis Rubber, Japan) of IX-850G and BARC of AZ KrF-12 (Clariant, Japan). The photoresist stripper was 1-methyl-2-pyrrolidone (NMP) from E. Merck (Germany).

All reagents used were of analytical or higher grade from E. Merck. High-purity water, which was purified by demineralization, two-stage quartz distillation, and subsequent subboiling distillation, was used throughout. Nitric acid (E. Merck, Darmstadt, Germany; Tracepure grade, further treated by in-house subboiling), sulfuric acid (Fisher Scientific, Pittsburgh, PA; Tracemetal grade), hydrogen peroxide (E. Merck), and hydrogen chloride (E. Merck) were used for digestion of the samples. Standard solutions of the analytes in 1% nitric acid were freshly prepared by the dilution of aqueous 1000mg/L stock solutions (E. Merck).

2.2 Film growing process

To prepare different underlying surfaces for this study, films of polysilicon, silicon oxide, and silicon nitride were deposited on various starting silicon wafers by low-pressure chemical-vapor-deposited (LPCVD) method in a quartz reactor. The polysilicon film was deposited with silane gas (SiH_4) in 60 sccm and 620°C . The silicon oxide layer was grown by wet oxidation with a mixture gas of hydrogen (8 slm) and oxygen (4999 sccm) at 978°C . While the silicon nitride film was deposited with a mixture gas of ammonium (130 sccm) and dichlorosilane (SiH_2Cl_2 , 30 sccm) at 780°C .

Afterwards, wafers were cut into 2 cm x 2 cm pieces to serve as test samples. Photoresist layer was then coated on the test samples. This was accomplished by first holding the test sample on the chuck by vacuum, and then 1 ml of radioactive DUV PR or BARC was dispensed on the sample surface by the pipette. The coating processes of DUV PR and BARC were performed by spinning at 1500 rpm for 0.5 min. Samples of DUV PR were then split to receive various baking at 80 and 120°C for 2 min by a hot plate, while BARC was baked at 180°C for 1 min.

2.3 Radioactive tracer experimental procedure

To prepare the radioactive DUV PR and BARC, one volume of radioactive tracer was mixed with five volume of lithographic materials, and the radioactive lithographic solution was well shaken to ensure homogeneous state. The radioactive lithographic solution was then applied to the test sample by the spin-coating process as mentioned above. After solvent evaporation, the test sample was counted by the high resolution gamma-ray spectrometer. The counting system consists of HPGe detector coupled with multi-channel analyzer (CANBERRA AccuSpec) and the usual electronics. The energy resolution of the system was 2.4 KeV for 1332 KeV. The intensity of gamma-ray for Cs ($t_{1/2}=30.15$ y) and Zn ($t_{1/2}=243.9$ d) was monitored at the energy of 661.7 and 834.8 KeV, respectively. After counting, the photoresist layer was removed by dipping in a 100 ml NMP solution at 60°C for 5 min, and then dried by hot plate. The radioactivity of impurities on the wafer was also checked by the HPGe detector. However, the counting time should be elongated to minimize the counting error. The diffusion ratio of Cs and Zn impurities from photoresist into the underlying substrate was determined by the ratio of the time-average counts from the underlying substrate and those from the photoresist coated onto the surface.

2.4 Microwave digestion and sample analysis

Microwave digestion of lithographic materials was accomplished with the use of two various types of commercial oven, namely closed-vessel and open-focused. The closed-vessel type of Model MDS-2000 (CEM, Matthews, NC) equipped with a Teflon-coated cavity and removable 12-position sample carousel. The oven has a variable power range (up to 630 W) adjustable in 1% increments. The existing turntable was rotated at 3.5 rev/min and a pressure line was installed with a transducer for pressure monitoring. The pressure limit was set at 150 psi (1 psi=6895 Pa), a gas pressure in the vessel over the setting pressure limit resulted in the power being turned off; when the pressure dropped to 148 psi, the power was restarted to heat the sample. The sample was digested in a lined digestion vessel (100ml volume, maximum operating pressure 200 psi) consisting of a chemically resistant inner liner (Teflon PFA) and cover to contain and isolate the sample solution from a higher strength outer pressure vessel body (Ultem polyetherimide). In order to protect the digestion vessel from excessive pressures, a rupture membrane (Part number 324350, CEM) was used to direct the escape gases through the exhaust port if the safety rupture membrane broke.

The open-focused microwave devices of Microdigest 3.6 (Prolabo, Paris, France) were composed of two PS-34 pumps, six microwave chambers, six temperature sensors, fume-scrubbing unit and the controlling console. Unlike the manual reagent introduction of CEM type oven, this system can automatically deliver the dissolution reagents (up to four) without the possibility of mixing. The reagent volume can be introduced from 0 to 99.5ml in 0.5ml increments. Because this digestion system was operated at atmospheric pressure, the dissolution process of each digestion chamber was independently controlled with the temperature setting by infrared-red monitoring from 100 to 400°C . The maximum power applied for each chamber was 250 W, and can be adjustable in 1% increments during 10 to 100%, or to zero power. The dissolution chamber and reflux condenser were made with high purity quartz.

0.25ml of lithographic material was digested in the closed-vessel microwave oven, and 3ml of sample was used in open-focused microwave system. The recipes of various acid mixtures or digestion programs were used to find the best dissolution condition. After digestion, the sample was cooled and transferred into another Teflon beaker. The sample solution was heat with the quartz hot plate on a clean bench (class 100) to evaporate to incipient dryness, and subsequent adding with 5ml of 1% nitric acid. The above solution can be used either for evaluating the completeness of the digestion process by UV-VIS spectrometry, or for the determination of the impurity using the ICP-MS (Perkin-Elmer Sciex Elan Model 5000, Norwalk, CT), GFAAS (Perkin-Elmer, Zeeman 5100PC) and ICP-OES (Perkin-Elmer, Optima 3000). The alternative method for evaluating the digestion efficiency was weighted the dry residual solid after sample digestion and reagent evaporation.

3. RESULTS AND DISCUSSION

3.1 Impurities Migration

In general, a basic lithographic process consists of resist coating, softbake, exposure, post exposure bake, development and hardbake. One of lithographic materials, DUV PR, can be used to define the pattern for critical layer. However, Bencher and co-workers²⁷ reported numerous problems, such as interference, reflective notching and standing waves, associated with proximity effects to be happened for only coating PR layer during exposure. Therefore, it needs to use BARC, which coated between the PR and the underlying layer, or TARC, which coated on the PR layer, to minimize the exposure problem. Since the impurity in the BARC or PR has the possibility to migrate into the substrate, it is extreme important to explore the diffusion behavior or mechanism for future development. Three possible mechanisms have been previously proposed for impurities existing in the silicon wafer during higher temperature process and cooling step²⁸. They include impurity precipitation, out-diffusion, and electrical activation by forming deep energy levels within the energy band gap of silicon. However, little has been reported about the behavior of metallic impurities in DUV PR and BARC of lithographic materials. The metallic impurities in the DUV PR and BARC should move in the free cation or ion-pair state during baking process. Once it out-diffuses into the interface between the coating layer and the underlying substrate, it is reasonable to assume that precipitation, gettering, and further diffusion into the underlying substrate are all possible. Even if the original impurity diffusion source is removed from the interface in the early stage of baking, subsequent diffusion of the remaining impurity near the interface may still be possible. The out-diffusion may continue until a steady state is reached between in- and out-diffusion.

Table 1 summarizes the diffusion ratios of Cs and Zn impurities from DUV PR and BARC into various underlying substrates for different baking temperatures (i.e., 180°C for BARC, and 80 and 120°C for DUV PR). It can be seen that the diffusion ratios seem to be higher for BARC than DUV PR except for the Zn on bare silicon case. Also, it is found that the diffusion ratios for DUV PR are all below 6%, irrespective of the underlying substrates and baking temperatures. This can be explained by the fact that both Cs and Zn in the DUV PR have low diffusion ability at the baking temperatures used in this study. Fig. 1(a) explained that only appreciable amounts of impurity in the interface (L in Fig. 1(a)) are mobile, while the concentration distribution (Ci in Fig. 1) of impurities in the bulk DUV PR layer does not seem to change during baking. But the BARC is not the same behavior, the larger diffusion ratios which illustrates in Fig. 1(b) imply the concentration profile of impurities in the longitudinal BARC layer should be changed during baking. Part of impurity in the BARC layer should be out-diffusion into the underlying substrate. The different diffusion behavior for the DUV PR and BARC can be explained by three possible reasons, i.e. the thin thickness of BARC (i.e. 750Å) as compared with PR (i.e. 7500Å), various material structures or different baking temperature. On considering the film porosity, the refractive index can be treated as a valuable indicator. The refractive index obtained at 248 nm for BARC layer (about 1.44) is significant lower than DUV PR layer (about 1.79). This explains the material structure of BARC layer is more porous, so the metallic impurities with any possible structure migrate easily within the porous structure. In addition to the effect of material structure, the baking condition is another decisive reason for impurity migration. However, up to now, it has no report to mention about the impurity diffusion in the lithographic layer. In order to describe the baking effect on impurity migration, the equation of diffusion coefficient, usually using to depict the impurity in the lattice, is applied in this study and presented in the following:

$$D = D_0 e^{\frac{-E_a}{kT}}$$

where D_0 is the pre-exponential factor dependent on the vibration frequency of atoms in the lattice or interstitial sites, T is the temperature in Kelvin, E_a is related to the height of the energy barrier at such sites, and k is the Boltzmann constant. It can predict from above equation that the diffusion coefficient for impurity in the BARC layer is higher than in DUV PR layer due to higher baking temperature.

Generally, the diffusion may be accelerated by elevating the reaction temperature. However, as can be seen from Table 1, the diffusion ratio does not depict strong temperature dependence for DUV PR at 80 and 120°C, respectively. This point would be illustrated in more detail in the following. Despite the appreciable amount of migrating impurity for DUV PR, it

shows different behaviors for different substrates. For example, the diffusion ratios of Zn impurity are 4.9 and 1.6 for the bare silicon substrate at baking temperature of 80 and 120°C, respectively. The film porosity obtained from the refractive index can not be used explain the above phenomenon because it shows the opposite trend. Also, the equation of baking effect, which was mentioned above, can not use to explain the diffusion behavior. In order to reveal the exact diffusion pathways for Cs and Zn in the photoresist layer, the microscopic and atomic structure in the boundary and DUV PR layer may be considered. However, this aspect was not investigated further.

Interestingly, Zn in the DUV PR does not exhibit any diffusion into the underlying silicon nitride. This can be explained by the surface structure of silicon nitride film. Silicon nitride film grown by LPCVD is very susceptible to water molecule adsorption from the air by forming N-H or Si-H bonds. The interaction force should be originated from the hydrogen bonding between the water molecule and the dangling bond of silicon nitride. The adsorbed water molecule on the surface of silicon nitride may be diffused into the PR layer during baking, and subsequently causing the Zn impurity to be solvated in the form of $Zn(H_2O)_x^{n+}$ by the water. The formation of the solvating complex has considerable size in the interface near the PR. Therefore, the diffusion ability for the impurity species should significantly decrease, and eventually stop. The following question then arises: Why should the nitrogen in silicon nitride film, which can form the pairs with the impurity, be diffused into the PR layer during baking. It is anticipated that the silicon nitride layer is usually deposited at a high temperature of 750-850°C, and the bond of silicon and nitrogen is definitely stable in the resist bake temperature. Hence, out-diffusion of nitrogen in such condition is not possible.

According to Table 1, similar result is observed only at 120°C for Zn impurity on silicon oxide case. As to the reason why Zn only diffuses at lower temperature of 80°C while not at 120°C, it is assumed that the extent of water desorption is different. Silicon oxide layer, which is deposited at a higher temperature of 950-1050°C, should be more stable than silicon nitride. The adsorption of water vapor from the air is minimized due to the lack of dangling bond on the silicon oxide surface. However, once some defects appear on the surface of amorphous silicon oxide, the water molecule would be adsorbed onto the surface. Our results demonstrate that the temperature for the vaporization of surface water adsorbed on silicon oxide can be achieved at 120°C. The water can quench the Zn impurity in DUV PR layer during the baking process. Moreover, similar behavior is also observed in the case of polysilicon underlayer. A native ultrathin oxide should appear on the polysilicon surface after exposing in the air. Therefore, the Zn impurity can be quenched at 120°C within the PR layer.

It should be noted that the diffusion ratios of Cs at baking with 120°C are higher than with 80°C for various underlying layers except silicon nitride. This is because the baking temperature plays an important role on impurity migration for underlying layers of bare silicon, polysilicon and silicon oxide. For the silicon nitride case, the diffusion ratio obtained at 80°C is higher than 120°C. This can be also explained by the surface structure of silicon nitride film as mentioned early. The adsorbed water molecule on the surface of silicon nitride may be diffused into the DUV PR layer during baking at 120°C, and subsequently causing the Cs impurity to be solvated in the form of $Cs(H_2O)_x^{n+}$ by the water. The formation of the solvating complex has larger size in the interface near the PR, and consequently, the diffusion ability for the impurity species should decrease.

3.2 Evaluation of Digestion Efficiency of Closed-vessel Method

Lithographic materials such as photoresist or anti-reflective coating material contain various types of polymers and organic compounds which maybe combine with the metallic impurities to form various complex compounds. On considering the purpose of material incoming quality control, the metallic impurity level is of prime importance. However, there existing numerous problems by direct sample introduction into analytical instrument. For example, the complex and viscous character of such material can serious clog the sample loop or interface of the measuring instrument, and affect the analytical reliability²⁹. To overcome the analytical problem, the proper sample pretreatment method is extreme important^{26,29}. The destruction of organic matter in the sample is usually to be used for trace and ultratrace analysis. However, to what extent the matrix is destroyed by a specific decomposition method has been so far seldom evaluated quantitatively. Conventionally, when clear and colorless solutions are obtained, or when total recovery of some elements is obtained, it has been assumed that oxidation of the organic matter has been completed for practical purposes. However, such assumptions are not necessarily reliable in all cases. More conclusive and direct information as to the presence and identities of residual matter retained by the acid dissolution is certainly desirable, especially if such matter might interfere in any subsequent measurement.

In this study both the UV/VIS spectrometric and gravimetric methods were tested for its applicability to evaluate the completeness of destruction of the sample matrix. Lithographic materials which contain various kinds of polymer and other organic compounds exhibit distinct absorption spectra in the UV/VIS region. Destruction of the organic matrix may, consequently, result in a decrease in the intensity of UV/VIS absorption, and the measurement of decreasing absorption of the digested sample can probably provide useful information to evaluate the effectiveness of sample decomposition. Fig. 2 shows the UV/VIS absorption spectra from 200 to 500 nm for KrF BARC and PR samples, prior to and after digestion by

closed-vessel method. Fig. 2(a) shows the BARC (diluted 1:10000) exhibits strong absorption at 200 to 240 nm, while the sample after one step closed-vessel microwave digestion with reagent mixture (HNO_3 and H_2O_2) and the program 1 as appeared in Table 2 exhibits the strong absorption between 200 and 220nm. This indicates that the digestion is not complete, and the residual pressure after digestion should be 60-70psi. But if the digestion is progressed with step 2 of 0.5mL H_2O_2 , only appreciably low absorption in the same wavelength region as shown in Fig. 2(a). This may provide a preliminary indication of the effectiveness of this digestion procedure for KrF photoresist sample. Fig. 2(b) depicts the UV/VIS absorption of the digest by the low power program 2. It is found that strong absorption below 220nm is still distinctive. This explains the program 1 in Table 2 is more powerful for BARC decomposition. Table 3 reveals the digestion efficiency of program 2 is lower than the most efficiency program 1 (near 100%). In addition, the digestion efficiency of step 1 can only achieve 89%. The somewhat positive correlation between the determination of digestion efficiency with dry residual method and the exhibiting absorbance of the digest sample may provide a feasible means to identify the extent of digestion condition.

Fig. 2(c) and (d) show the UV/VIS absorption spectra from 200 to 500nm for PR sample. It is found that the intense absorption of 200-220 and 300-400nm is still existed irrespective of only step 1 or two steps digestion procedure by program 1. However, Table 3 demonstrates the digestion efficiency is 91.2 and 99.5 for only 1 and two steps digestion. Therefore, the two steps digestion by program 1 seem to be very effective for PR sample. As can be seen from Fig. 2(d) and Table 3, the program 2 behaves poor digestion efficiency as compared with program 1.

3.3 Evaluation of Digestion Efficiency of Open-focused Method

Unlike the small sample size used in the closed-vessel method mentioned previously, the open-focused microwave method can adopt the large sample size up to 10g. In this work, the 3ml of lithographic material is tested with various acid mixtures to evaluate the digestion efficiency. Fig. 3 demonstrates the UV/VIS absorption spectra for KrF BARC and PR. It should be found from this figure that the remarkably high absorption was observed at 200 to 500nm. However, it can be seen from Fig. 3(a) and (b) that, after the digestion procedure of recipe 1, the majority of the absorption spectra disappears but a broad and low intense absorption at lower than 250nm still remains. In the same figure, it is interesting to found that recipe 2 with HNO_3 and H_2SO_4 mixtures may not digest more efficiency than recipe 1.

To verify the existing UV/VIS broad absorption is not serious in impurity determination, the dry residual method is also used to reflect the digestion efficiency. Table 4 listed the gravimetric result, which indicated the recipe 1 was the most efficient method for the destruction of various lithographic materials. Most of the matrix except for i-line resist was destroyed in the first step of recipe 1. It should be found that about 73% of digestion efficiency was achieved for only using digestion procedure of step 1 in i-line resist. By following with the digestion procedure of step two, the digestion efficiency can be enhanced to near 96.3%. It was also found that recipe 2, which replaced 5ml HNO_3 with 5ml H_2SO_4 , can also maintain the high digestion efficiency. But in practical use, numerous literatures report the H_2SO_4 can lead serious problem in ICP-MS determination, and this recipe was not suggested. Therefore, recipe 1 is most proper in lithographic material digestion than other recipes appeared in this table. This table also demonstrated digestion with reverse aqua regia and H_2O_2 in the step 1 of recipe 3 was significant superior than the using of aqua regia and H_2O_2 of recipe 4. It should be explained the oxidizing power of HNO_3 play an important role in lithographic material decomposition than the using HCl .

3.4 Analysis of Lithographic Materials

The analytical performance of the closed-vessel and open-focused microwave digestion and ICP-MS determination method was evaluated in terms of detection sensitivity, spike recovery and analytical reliability. The method detection limits as shown in Table 5, defined as the analyte concentration that gives a signal intensity which is three times the standard deviation of the procedure blank ($n=7$), were estimated to be. It can be found that the method detection limits of the closed-vessel method is lower than the open-focused method, irrespective the sample size of the closed-vessel is lower. It was also found that the absolute blank of the open-focused method was higher than closed-vessel method for analytes. The higher blank of the open-focused system can be attributed to the large reagent use and the open environment.

Recovery tests were performed by spiking equivalent amounts of 5ppb concentration of analyte to the closed- and open-focused vessel for lithographic materials, followed by the digestion sequence and determination method of the proposed method. The results of the spike recovery test for these elements are shown in Table 6. As can be seen, the spike recoveries of closed-vessel method for the analytes except Ca ranged in 87-125, 91-132, and 89-131 for the KrF, BARC, and i-line samples, respectively. The recovery of Ca is not performance well due to the isobaric interference from the carrier gas of argon in ICP-MS detection. More, the spike recoveries of open-focused method for the analytes except Ca ranged from 88 to 121, 82 to 119, and 82 to 112 for the various samples. This indicates the feasibility of applying the closed-vessel and open-focused microwave digestion procedure and ICP-MS multielement determination method to lithographic materials.

The proposed method has already been applied to the determination of multielement in semiconductor lithography

samples. Table 7 shows the analytical results with various digestion procedure. Those data obtained from mutual digestion methods seems to be very close, indicating the accuracy of the established methods. In addition, the relative standard deviation (RSD) as appeared in Table 7 is within 15%, which reveals the analytical results are all in reasonably good precision. Despite no commercial certified reference samples can be found, those data provided in Table 7 insure the reliability of the proposed closed-vessel and open-focused methods.

ACKNOWLEDGMENT

The authors thank the National Science Council, Taiwan, for financially supporting this research through contract #NSC88-2722-2317-200.

REFERENCES

1. S. M. Sze, VLSI Technology, McGraw-Hill, New York, pp.623, 1988.
2. C. Y. Chang and S. M. Sze, ULSI Technology, McGraw-Hill, New York, pp.680, 1996.
3. P. J. Ward, *J. Electrochem. Soc.*, **129**, pp.2573, 1982.
4. M. Miyazaki, M. Sano, S. Sumita and N. Fujino, *Jpn. J. Appl. Phys.*, **30**(2B), pp.L295, 1991.
5. A. L. P. Rotondaro, T. Q. Hurd, A. Kaniava, J. Vanhellefont, E. Simoen, M. M. Heyns and C. Claeys, *J. Electrochem. Soc.*, **143**, pp.3014, 1996.
6. F. H. Dill, W. P. Hornberger, P. S. Hauge and J. M. Shaw, *IEEE Trans. Electron Devices*, **ED-22**, pp.445, 1975.
7. D. J. Kim, W. G. Oldham and A. R. Neureuther, *IEEE Trans. Electron Devices*, **ED-31**, pp.1730, 1984.
8. C. A. Mack, *J. Electrochem. Soc.*, **134**, pp.148, 1987.
9. The National Technology Roadmap for Semiconductors, Semiconductor Industry Association, pp.93, 1997.
10. J. Schram, *Fresenius J. Anal. Chem.*, **343**, pp.727, 1992.
11. L. Fabry, S. Pahlke, L. Kotz and G. Tolg, *Fresenius J. Anal. Chem.*, **349**, pp.260, 1994.
12. F.-H. Ko and M.-H. Yang, *J. Anal. At. Spectrom.*, **11**, pp.413, 1996.
13. J. S. Crighton, J. Carroll, B. Fairman, J. Haines and M. Hinds, *J. Anal. At. Spectrom.*, **11**, pp.R461, 1996.
14. G. R. Fuchs-Pohl, K. Solinska and H. Feig, *Fresenius J. Anal. Chem.*, **343**, pp.711, 1992.
15. M. D. Argentine and R. M. Barnes, *J. Anal. At. Spectrom.*, **9**, pp.1371, 1994.
16. M. B. Shabani, T. Yoshihiro and H. Abe, *J. Electrochem. Soc.*, **143**, pp.2025, 1996.
17. M. G. Dowsett, R. D. Barlow and P. N. Allen, *J. Vac. Sci. Technol.*, **B12**, pp.186, 1994.
18. R. J. Borg and G. J. Dienes, *An Introduction to Solid State Diffusion*, Academic Press, CA, pp.255, 1988.
19. I. P. Glekas, *Water Sci. Technol.*, **32**, pp.179, 1995.
20. G. R. Choppin and J. Rydberg, *Nuclear Chemistry*, Pergamon Press, Oxford, pp.425, 1980.
21. W. Kern and D. A. Puotien, *RCA Rev.*, **31**, pp.187, 1970.
22. M. Takenaka, S. Kozuka and Y. Hashimoto, *Bunseki Kagaku*, **42**, pp.71, 1993.
23. E. H. Evans and J. J. Giglio, *J. Anal. At. Spectrom.*, **8**, pp.1, 1993.
24. H. M. Kingston, *Atomic Spectro.*, **19**, pp.27, 1998.
25. F. E. Smith and E. A. Arsenault, *Talanta*, **43**, pp.1207, 1996.
26. C.-C. Huang, M.-H. Yang and T.-S. Shih, *Anal. Chem.*, **69**, pp.3930, 1997.
27. C. Bencher, C. Ngai, B. Roman, S. Lian and T. Vuong, *Solid State Technol.*, Mar., pp.109, 1997.
28. K. Graff, *Metal Impurities in Silicon-Device Fabrication*, Springer, Berlin, pp.7, 1995.
29. K. E. Jarvis, A. L. Gray and R. S. Houk, *Handbook of Inductively Coupled Plasma Mass Spectrometry*, Chapman and Hall, NY, 1992.

Table 1. The diffusion ratio for impurities transported from DUV BARC and photoresist into underlying substrates at various baking temperatures.

substrate	element	BARC	PR	PR
		180°C, %	80°C, %	120°C, %
bare silicon	Cs	20.0	1.9	2.9
	Zn	0	4.9	1.6
polysilicon	Cs	46.2	0.9	3.1
	Zn	25.8	2.3	0
silicon oxide	Cs	13.4	0.7	1.4
	Zn	35.5	5.6	0
silicon nitride	Cs	17.3	3.9	2.6
	Zn	26.2	0	0

Table 2. Microwave program for closed-vessel digestion.

program 1				program 2			
step	power (%)	time (min)	pressure limit (psi)	step	power (%)	time (min)	pressure limit (psi)
1	40	30	150	1	35	30	100
2	55	30	150	2	35	30	100

Table 3. Effect of digestion efficiency of various recipes with dry residual method for lithographic materials after closed-vessel microwave digestion.

Sample	BARC,%	PR,%
program 1	100	99.5
program 1* ¹	89.0	91.2
program 2	92.0	94.3

*The sample volume is 0.25ml. The digestion recipe has two steps, where the reagent for first step is 1.5ml HNO₃ and the reagent for second step is 0.5ml H₂O₂. Detailed procedures for program 1 and 2, see Table 2.

¹only digestion with the first step of program 1.

Table 4. Effect of digestion efficiency of various recipes with dry residual method for lithographic materials after open-focused microwave digestion.

Sample	KrF PR,%	BARC,%	i-LINE,%
recipe 1	99.6	99.8	96.3
recipe 1* ¹	97.2	96.5	73.0
recipe 2	94.9	97.9	-
recipe 3	96.7	99.8	-
recipe 4	78.7	97.0	-

*The sample volume is 3ml and the digestion program is mentioned in experimental section. Recipe 1: step 1 is 10ml HNO₃ and 3ml H₂O₂, and step 2 is 5ml HNO₃ and 5ml H₂O₂. Recipe 2: step 1 is 5ml HNO₃, 5ml H₂SO₄ and 3ml H₂O₂, and step 2 is 5ml HNO₃ and 5ml H₂O₂. Recipe 3: step 1 is 9ml HNO₃, 3ml HCl and 3ml H₂O₂, and step 2 is 5ml HNO₃ and 5ml H₂O₂. Recipe 4: step 1 is 3ml HNO₃, 9ml HCl and 3ml H₂O₂, and step 2 is 5ml HNO₃ and 5ml H₂O₂.

¹only digestion with the first step of the recipe.

Table 5. Method detection limits of lithographic materials digested by closed-vessel and open-focused microwave method, and determined by ICP-MS and ICP-OES

Element	ICP-MS, ppb		ICP-OES, ppb	
	closed-vessel	open-focused	closed-vessel	open-focused
Na	3.99	84	12.8	206
Al	0.55	20.0	2.3	15.9
Ca	19.6	44.9	2.3	4.5
Cr	1.13	0.74	1.6	1.2
Fe	7.89	10.2	3.3	3.9
Ni	0.21	0.39	4.1	2.4
Cu	0.10	0.39	2.6	2.4
Zn	0.79	1.28	2.8	4.8
Au	0.71	0.57	1.5	3.6
Pb	0.10	0.22	6.6	4.1
Sn	0.65	4.04	14.3	14.2
Pt	0.04	0.28	5.9	5.7
Cs	0.08	0.10	-	-

*The method detection limits are based on three times the standard deviation of the procedure blank (n=6).

Table 6. Spike recoveries (%) of lithographic materials digested by closed-vessel and open-focused microwave digestion, and determined by ICP-MS

Element	closed-vessel		open-focused	
	PR	BARC	PR	BARC
Na	98	132	118	102
Al	100	121	121	119
Ca	187	142	146	125
Cr	87	91	97	110
Fe	117	127	92	99
Ni	125	110	100	82
Cu	100	107	101	87
Zn	106	116	103	100
Au	103	111	88	99
Pb	109	108	92	113
Sn	89	97	108	91
Pt	88	104	97	90
Cs	112	101	100	104

Table 7. Analytical results of lithographic materials digested by closed-vessel and open-focused digestion, and determined by ICP-MS

Element	closed-vessel		open-focused	
	PR	BARC	PR	BARC
Na	298±3	166±7	343±10	155±14
Na ^a	280±18	169±3	387±38	146±17
Al	3.12±0.18	151±4	3.63±0.36	172±61
Al ^a		161±6		178±63
Ca	76.1±3.9	169±40	192±60	292±17
Cr	7.9±0.6	1.95±0.31	8.7±1.1	1.90±0.34
Fe	7.36±1.21	7.62±0.90	7.19±2.2	6.92±1.93
Ni	1.08±0.06	1.01±0.24	1.07±0.67	0.64±0.07
Cu	2.55±0.16	1.56±0.21	3.27±0.22	1.65±0.42
Zn	2.09±0.31	4.16±0.26	2.20±0.15	4.50±1.56
Au	12.1±0.9	5.53±0.67	13.2±3.2	5.38±0.66
Pb	0.021±0.005	ND	ND	ND
Sn	5.79±0.53	0.51±0.02	6.14±1.36	0.65±0.18
Pt	0.006±0.001	ND	ND	ND
Cs	ND	ND	ND	ND

a. determine by ICP-OES method

b. ND = not detected

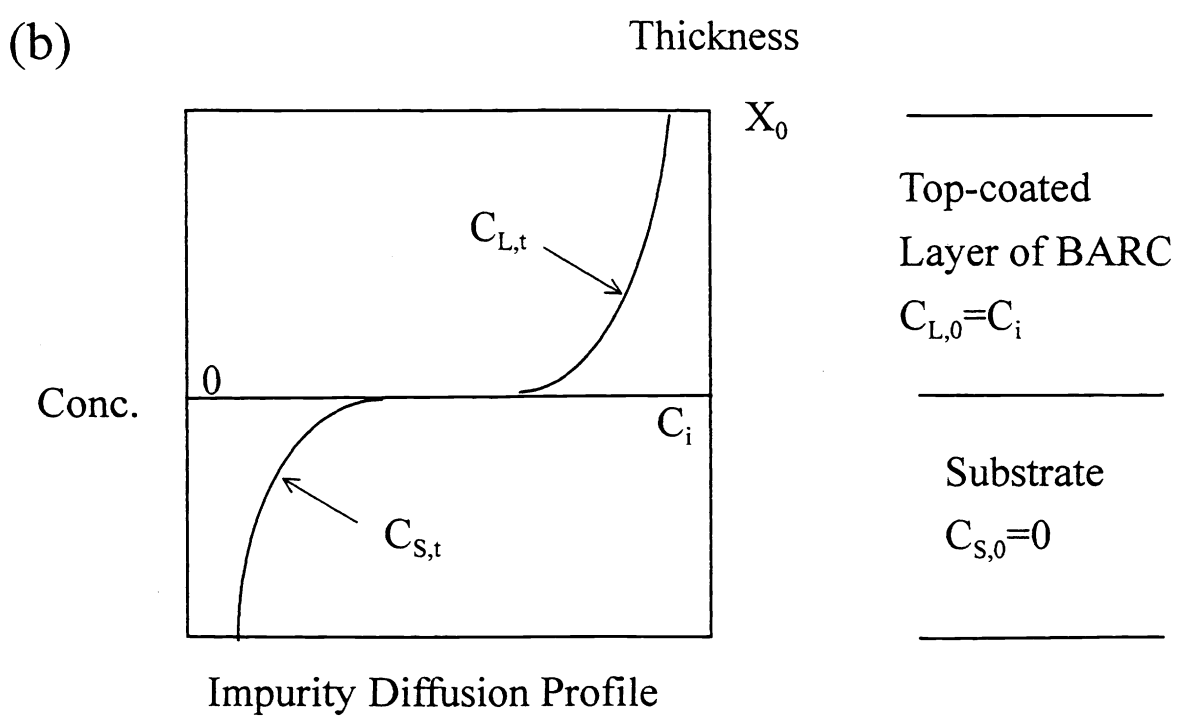
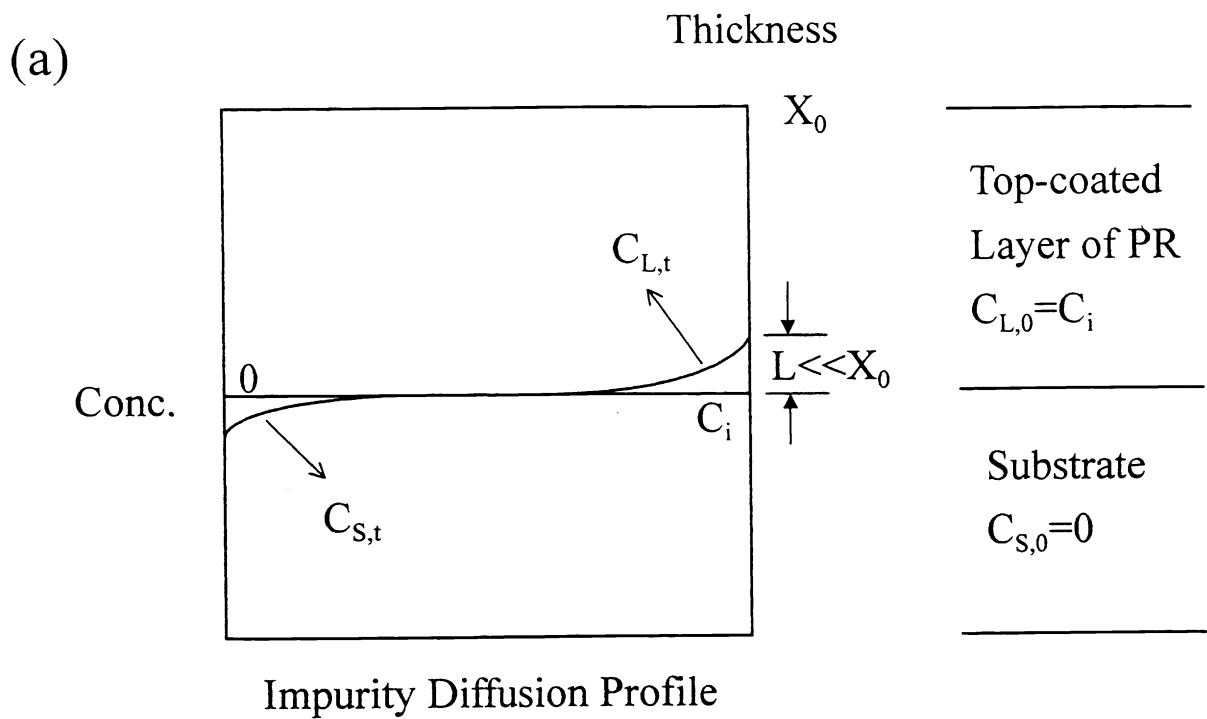


Fig. 1 Impurity diffusion profile of (a) KrF PR sample; and (b) BARC sample.

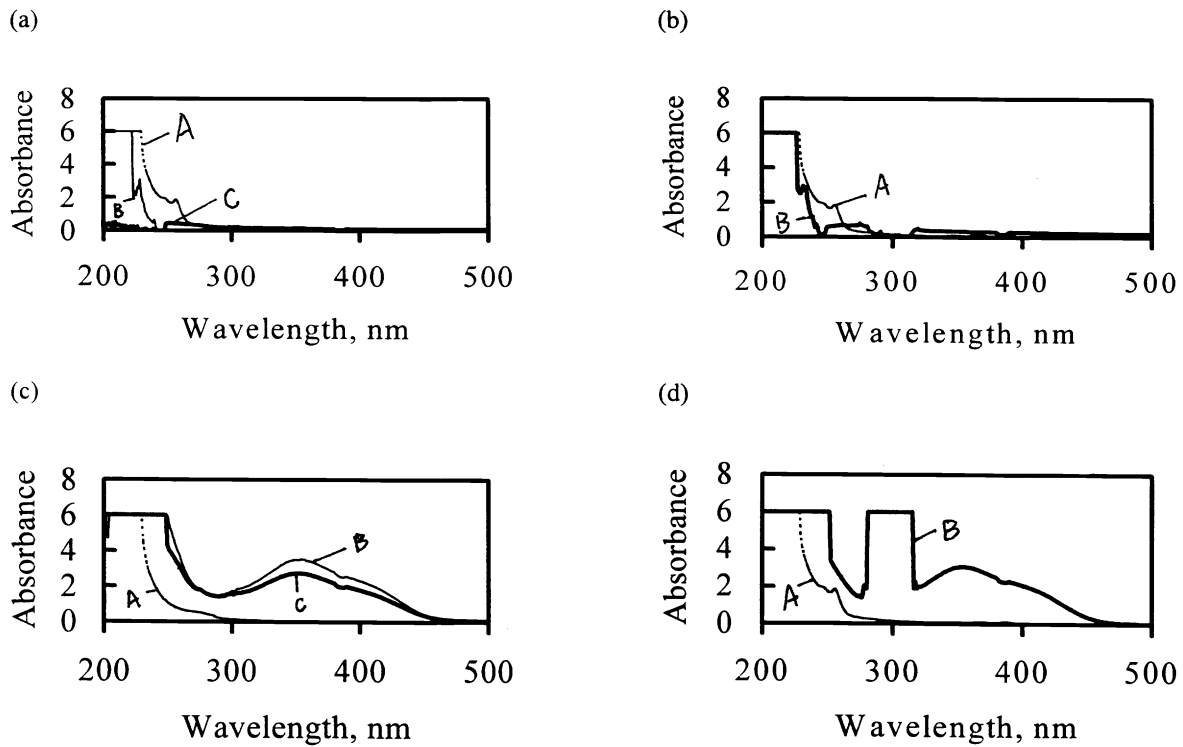


Fig. 2 UV/VIS absorption spectra of close-vessel digestion of (a) BARC samples, where A is original BARC (1:10000 dilution), B is BARC sample after step 1 of program 1 digestion (1: 500 dilution) and C is BARC after program 1 digestion (1:60 dilution); (b) BARC samples, where A is original BARC (1:10000 dilution) and B is BARC after program 2 digestion (1:300 dilution); (c) KrF PR samples, where A is original PR (1:10000 dilution), B is PR after step 1 of program 1 digestion (1:200 dilution) and C is PR after program 1 digestion (1:60 dilution); and (d) PR sample, where A is original PR (1:10000 dilution) and B is PR after program 2 digestion (1:100 dilution).

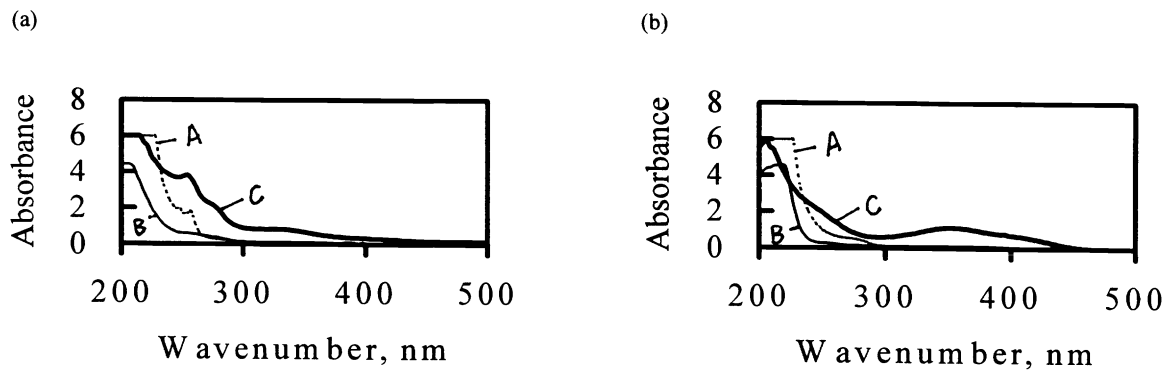


Fig. 3 UV/VIS absorption spectra of open-focused digestion of (a) BARC samples, where A is original BARC (1:10000 dilution), B is BARC after recipe 1 digestion (1:400 dilution) and C is BARC after recipe 2 digestion (1:400 dilution); and (b) KrF PR samples, where A is original PR (1:10000 dilution), B is PR after recipe 1 digestion (1:1000 dilution) and C is PR after recipe 2 digestion (1:1000 dilution).